Long Josephson junctions driven by biharmonic signals

G. Filatrella
Physikalisches Institut, Lehrstuhl Experimentalphysik II, Auf Der Morgenstelle 14, Universität Tübingen, D-72076 Tübingen, Germany
and Department of Physics, University of Salerno, I-84081 Baronissi, Italy

G. Rotoli
Department of Energetics, University of L'Aquila, Localita' Monteluco I-67040, Roio Poggio (AQ), Italy
(Received 13 April 1994)

Biharmonic-driven long Josephson junctions are studied within the framework of a perturbative approach for the motion of fluxons in the junctions. A thorough study of phase-locking states is carried out giving a generalization of the phase-locking conditions valid for any type of periodic external drive. These conditions give rise to a classification of phase-locked steps on the current-voltage characteristics of the junction. Enhancement of dynamical phase-locked regions and stabilization in connection with the phenomenon of chaos suppression are two interesting characteristics of biharmonic phase-locking states. Numerical simulations show that the theoretical predictions are, in general, well reproduced.

I. INTRODUCTION

The driven Josephson junction is an interesting device both for practical applications as a voltage standard or a local oscillator[1] or for theoretical investigations in nonlinear dynamics.[2] Its basic feature is that it makes possible a current-controlled tunable oscillator in the GHz range. Under certain conditions, oscillations can phase lock to the external drive;[3,4] in the phase-locked (PL) state the period of the nonlinear oscillation has a rational relationship with the period of the external drive. The phase between the two oscillations can adapt to a change in the bias current so that the period of the nonlinear oscillator can become independent of the bias current; this gives, via the standard Josephson relations,[5] a current singularity, i.e., a constant voltage-current step on the I-V current-voltage characteristic of the junction. Such dynamical regions are commonly observed in experiments, and are often referred to as phase-locked steps.[1] PL states can be reproduced in the analytical model and numerical simulations of Josephson junctions, by assuming that the external signal is an harmonic signal of type $\eta(t) = \eta_0 \sin \omega t$;[4,6] this is sufficient in many cases to produce an excellent agreement with the experimental data (for example see Ref. 6).

Progress in the development of practical devices is related to the possibility of obtaining large and stable phase-locked steps in order to maximize the effect of mutual locking between junctions.[7] In the case of small junctions the analysis of Monaco[8] shows that a biharmonic signal, i.e.,

$$\eta(t) = \eta_0 \sin(\omega t) + \eta_1 \sin(\sigma \omega t + \psi), \qquad (1)$$

can, in some cases, give an enhancement of dynamical regions of phase locking (PL). Monaco's results can be summarized as follows: (i) A larger dynamical region and a larger stability can be obtained using biharmonic signals; (ii) experiments performed with $\sigma = 2$ and $\psi = \pi/4$ [see Eq. (1)] are in good agreement with the theory; (iii) experimentally it was noted that chaos, arising in the system for some values of parameters, was partially suppressed.

More recently theoretical work in connection with chaos suppression due to the presence of biharmonic signals has been developed.[9–12] Chaos in Josephson systems is a well-known phenomenon in both small[13] and long junctions. In the latter case chaos can affect the system either as turbulence[14–16] (space and temporal chaos) or as temporal chaos (chaotic propagation of localized nonlinear oscillations in the junction).[17–20] Temporal chaos might destroy the PL state with features that are very reminiscent of small junction chaotic behavior. A natural problem is therefore how to eliminate such undesirable effects due to chaos. In the context of Josephson devices the so-called Ott-Grebogi-Yorke (OGY) methods,[21] which require a knowledge of the time-dependent dynamics and fast control of a tunable parameter, are not applicable.[11] Alternatively, the use of a weak periodic signal to control the chaotic dynamics is of simpler application;[22] it was also proved to be effective for short Josephson junctions by direct numerical simulations.[11] The same authors have shown, with a simple model of the Poincaré map, that small and periodic signals are expected to decrease the maximum Liapunov exponent.

For a simplified model of the driven long Josephson junction (LJJ), Salerno has analytically proved that the first bifurcation of the Feigenbaum cascade can be shifted upwards by introducing a second subharmonic, leading to the disappearance of chaos.[12] Moreover, Filatrella *et al.*[23] have performed extensive simulations on the same system and have shown that (i) chaos can be suppressed also in the full model (the so-called perturbed sine-Gordon

equation) and the results are in good agreement with the simpler analysis; (ii) there exists a rich behavior depending on the choice of the subharmonic order; (iii) in some cases the second term is ineffective in suppressing chaos. There is therefore a first problem left unsolved: Is it possible to predict the effectiveness of the second term, depending both on the subharmonic order and the amplitude, in suppressing chaos?

Monaco has suggested that other signals, such as pulse train, can be used to obtain PL states,[8] and so a second question then arises: Is it possible to obtain, also in the LJJ case, phase-locked solutions which drive the system with different wave forms? This question is relevant also because pulse trains play a role in the reciprocal phase locking of LJJ (Ref. 7) since they simulate the signal emitted by the junctions.

In view of such interesting features the possibility of a biharmonic drive in the LJJ is investigated in the following under very general assumptions about the PL state: A generalized PL condition is stated and its consequence for the fluxon dynamics is explored in some typical cases.

We will show that PL exists in a class of situations which show both a periodic doubling route and chaotic motions of fluxons and/or multi-time-of-flight solutions (nTOF). We have explored also the possibility of using different wave forms in order to obtain PL solutions and have tried to find an answer also to the question concerning the prerequisites for obtaining chaos suppression in the LJJ simplified model. PL states, introduced with both biharmonic drive and general wave forms, can have in some cases very complicated dynamical features, for example, coexistence of more fixed points with a chaotic basin of attraction and chaotic behavior at all values of amplitude. A consequence of the first point would be that if the system is moved apart from the phase-locked condition (due to noise entering into the system) it is driven into an unstable or chaotic orbit.

The paper is organized as follows: In Sec. II we briefly describe the mathematical model of a LJJ; in Sec. III we state the general phase-locking conditions for arbitrary systems driven by periodic signals; in Sec. IV we study the existence of the periodic solutions for the LJJ system and their signature on the I-V characteristic; in Sec. V the stability of these solutions is analyzed and compared with numerical results; some conclusions are collected in Sec. VI.

II. MODEL

We model the LJJ fluxon oscillator as an in-line geometry junction, where external signals and the bias current enter only through the boundaries. The perturbed sine-Gordon equation describing the in-line geometry junction is (subscripts denote partial derivatives as usual):

$$\phi_{xx} - \phi_{tt} - \sin\phi = \alpha\phi_t - \beta\phi_{xxt}, \tag{2}$$

with time-dependent boundary conditions

$$\phi_x(0,t) + \beta\phi_{xt}(0,t) = -\chi + \eta(t), \tag{3a}$$

$$\phi_x(l,t) + \beta\phi_{xt}(l,t) = \chi + \eta(t). \tag{3b}$$

Distances are normalized to λ_J (the Josephson penetration length), and times to $\omega_J^{-1} = \lambda_J/\bar{c}$, the inverse plasma frequency, where $\bar{c}$ is the speed of light in the junction; α and β are loss parameters, and χ is the normalized bias current supplied to the junction. In Eqs. (3) $\eta(t)$ is the time-dependent term of the boundary conditions, i.e., the normalized external signal at the edges of the junction.[5] This signal can be due to the external ac magnetic field or to an ac current flowing in a narrow region close to the edges. In the first case the sign of the magnetic field is the same at both edges (magnetic coupling), whereas in the latter case it reverses (electric coupling).

It is well known that Eqs. (2) and (3) can sustain the motion of localized solutions that carry a magnetic flux quantum (and are therefore often referred to as fluxons). The motion of such solutions can be phase locked to the external signal[3,6] yielding the phenomena of phase-locking steps on the I-V characteristic of the junction. For relatively large values of the amplitude of the external signal the PL state can be destroyed by chaos which affects the system as (generally speaking) temporal chaos: The motion of flux quanta in the junction becomes chaotic without loss of the spatial coherency.[20]

Our main purpose is to study a LJJ driven by the time-dependent signal Eq. (1) for arbitrary values of σ. We first assume that $\eta_1 < \eta_0$ and define as *subharmonic* a signal with $\sigma < 1$, and otherwise as *superharmonic* a signal with $\sigma > 1$. Next we choose $\psi = 0$. This choice is different both from the Monaco small junctions case[8] and Salerno:[12] We prefer such a choice because for $\psi = 0$ the signal is symmetric and the comparison with previous literature on temporal chaos in a LJJ is straightforward.[19,20,23]

We will consider also some other functional forms for $\eta(t)$: square wave, triangular wave, and some kinds of pulse train; actually, only a pulse train appears to be a feasible experimental wave form.[8]

To investigate the properties of phase-locking states we utilize the perturbative approach used in Ref. 4 to describe the dynamics of fluxons in a LJJ. Such an approach is based on the McLaughlin-Scott perturbation scheme:[25] In this scheme the fluxon is described only by its position and velocity in the junction. For this reason the method is often referred to as the collective coordinate approach. This approach leads to the following map in terms of the variables t_p (the time variable of the fluxon after the pth reflection at a boundary) and y_p (the energy at the pth boundary):[26]

$$t_{p+1} = t_p + \frac{1}{a}\ln\left[\frac{u_p}{Cu_p - S}\right], \tag{4a}$$

$$y_{p+1} = \left\{\frac{(1-\lambda)(Cu_p - S)^2 + 1 - (1-\lambda)u_p^2}{1 - (1-\lambda)u_p^2 - \lambda(Cu_p - S)^2}\right\}^{1/2} + \frac{\pi}{2}[\chi + (-1)^{pm}\eta(t_{p+1})], \tag{4b}$$

where u_p is the velocity of the fluxon at the pth reflection:

$$u_p = \sqrt{1 - \frac{1}{y_p^2}}. \tag{4c}$$

In Eqs. (4) $a = \alpha + \beta/3$, $\lambda = (\beta/3)/(\alpha + \beta/3)$, $C = \cosh(al\sqrt{1-\lambda})$, and $S = \sinh(al\sqrt{1-\lambda})/\sqrt{1-\lambda}$. The variable m is set to 0 in the case of electric coupling, and to 1 in the case of magnetic coupling.[4] Here $1/a \ln[u_p/(Cu_p - S)]$ is the time of flight (TOF) of a fluxon defined as $T_{p+1} = t_{p+1} - t_p$, i.e., the time employed by the fluxon to propagate between the ends of the LJJ for a given initial velocity u_p. The first term of the right-hand side (RHS) of Eq. (4b) represents the final (reduced) energy of the fluxon after crossing the junction; the second term is the energy furnished by the external bias and field.

The agreement between this simplified approach and the full partial derivative equation (PDE) model is also satisfactory in the case of a biharmonic drive.[23]

III. GENERAL PHASE-LOCKING CONDITIONS

Let us assume that fluxons propagate in the junction with a succession of (in principle) different TOF. Each PL state must satisfy the condition that after nTOF the energy input from the external signal and the initial velocity of the fluxon will repeat, no matter what the details of the dynamics governing the propagation of the fluxon through the junction are. Therefore phase locking can be realized with external signals if after a sequence of nTOF the signal has the same phase; this gives to the oscillator exactly the same energy and thus starts another cycle of nTOF. To find explicitly this condition we fix the average TOF to be T, i.e., $nT = \sum_{k=1}^{n} T_k$, where the T_k's are the TOF of nTOF solutions (so the voltage on the I-V current-voltage characteristic of the junction will be $V = 2\pi/T$). In terms of a generic signal $\eta(t)$ this condition reads simply

$$\eta(nT + t) = (-1)^{mn}\eta(t). \tag{5}$$

This relation for the biharmonic signal [Eq. (1)] gives the conditions for ω and σ that can realize a PL state. These are, for electric and magnetic coupling cases, respectively,

$$\eta_0 \sin(\omega nT + \theta) + \eta_1 \sin(\sigma\omega nT + \sigma\theta) = \eta_0 \sin(\theta) + \eta_1 \sin(\sigma\theta), \tag{6a}$$

$$(-1)^n\eta_0 \sin(\omega nT + \theta) + (-1)^n\eta_1 \sin(\sigma\omega nT + \sigma\theta) = \eta_0 \sin(\theta) + \eta_1 \sin(\sigma\theta). \tag{6b}$$

Here θ is the phase relation between the signal and the fluxon oscillator (the use of θ rather than t avoids the continuous increase of the latter variable, mapping the essential information, i.e., the phase relation θ, onto a circle). Equations (6) are identities in the electric and n-even magnetic coupling cases if

$$\omega = l\frac{2\pi}{nT} = \frac{l}{n}V, \tag{7a}$$

$$\sigma = k\frac{2\pi}{\omega nT} \Rightarrow \sigma = \frac{k}{l}, \tag{7b}$$

and for n-odd magnetic coupling cases if

$$\omega = (2l+1)\frac{\pi}{nT} = \frac{2l+1}{2n}V, \tag{8a}$$

$$\sigma = (2k+1)\frac{\pi}{\omega nT} \Rightarrow \sigma = \frac{2k+1}{2l+1}. \tag{8b}$$

Only certain rational values of σ are allowed in the magnetic case with an odd number of TOF. Conversely, if we fix the frequency of the two biases, only solutions for certain values of n are allowed.

For example, in the case of Ref. 23 with $\omega = 3V/2$ and $\sigma = 1/2$ (magnetic coupling), we obtain $V/\sigma\omega = 4/3$; thus $n = 4$ is the lowest number allowed, and in fact this is also the lowest number of TOF observed in both PDE and map simulations. In particular the 1TOF solutions rules are the following:

(i) Electric coupling case: the frequency has to be an integer harmonic of the voltage ($\omega = lV$), and $\sigma = k/l$.

(ii) Magnetic coupling case: $\omega = V(2l+1)/2$, and $\sigma = (2k+1)/(2l+1)$, only odd steps exhibit 1TOF solutions in the magnetic coupling case. In particular we note that in the case $\sigma = 1/2$ the 1TOF cannot be realized.

If phase locking is realized with different wave forms, the mechanism of PL will be exactly the same; in deriving Eqs. (7) (8) we have not made use of the fact that the actual form is sinusoidal, only its periodicity.

Finally we note that the details of the dynamics cannot influence the phase-locking conditions. It is clear that such conditions must be fulfilled in order that the system restarts another cycle after a certain number of oscillations, but not sufficient, because the details of the range of existence and/or the stability of the PL solutions depend evidently on the actual form of the system for any oscillator phase locked to a biharmonic signal. In Ref. 8 the system was a small Josephson junction driven by a biharmonic signal which in our notation is described by simply taking $\sigma = j$, $k = j$, $l = 1$, $n = 1$, $m = 0$, $j = 2$ for the experimental data. On the other hand, the enhancement of PL ranges found by Monaco clearly depends on the small junction dynamical behavior.

IV. RANGE OF EXISTENCE OF nTOF SOLUTIONS

So far we have studied the conditions of periodicity of the external drive; we will now derive the range of existence of the PL states in the map, i.e., Eqs. (4). The signature of PL states for this system is current steps on the I-V characteristic that appear at voltage $V = 2\pi/T$. We report some typical cases in Table I. ω is chosen in

order that all the steps appear at the same voltage V.

In the following we will refer to the different phase-locking steps with the symbols used in the first column of this table. To simplify the problem we start with the 1TOF solution. In this case the PL state exists if there exists a value of θ such that a stationary bias level can be reached; i.e., after each flight across the junction the fluxon recovers the same energy from the stationary bias current plus the external signal (cf. previous section):

$$\chi + \eta_0 \sin(\theta) + \eta_1 \sin(\sigma\theta) = \chi_0 \tag{9}$$

(here, $0 \leq \theta \leq 2\pi l$, and χ_0 is the dc bias at the center of the step, i.e., where the free-running shuttling period coincides with the period of the PL solution). The extension of the step is then given by the maximum value that the sum of the two sine terms can achieve.

The fixed points can also be found explicitly by imposing the condition $t_{p+1} - t_p = T$ and inverting the first equation of the map in order to find y; then the other variable θ can be found by inverting Eq. (9). In Fig. 1 we report some typical ranges of existence of the single and multiple TOF solutions obtained simulating Eqs. (4) for the cases of Table I.

For 2TOF solutions we have to find the values of χ such that the following equations can be satisfied (for the electric coupling):

$$\eta_0 \sin(\theta) + \eta_1 \sin(\sigma\theta) = A(\chi, 2T - T_1), \tag{10a}$$

$$\eta_0 \sin(\omega T_1 + \theta) + \eta_1 \sin(\sigma(\omega T_1 + \theta)) = A(\chi, T_1), \tag{10b}$$

for $0 \leq \theta \leq 2\pi l$, and $T/2 \leq T_1 \leq 2T - L$; $A(\chi, t)$ is the function derived from Eq. (4b) as

$$A(\chi, t) = \frac{2}{\pi}\left\{ y(t) - \left[\frac{(1-\lambda)[Cu(t) - S]^2 + 1 - (1-\lambda)u(t)^2}{1 - (1-\lambda)u(t)^2 - \lambda[Cu(t) - S]^2} \right]^{1/2} \right\}. \tag{11}$$

$A(\chi, t)$ represents the energy that has to be furnished by the external signal to achieve a certain value of the time of flight [in this formula $y(t)$ and $u(t)$ represent the energy and the velocity of the fluxon at a time t after the reflection, respectively]. The zeros of these equations give the two t coordinates of the two fixed points (θ and the first time T_1), and the y coordinates can be found by inverting Eq. (4a). For the magnetic case the procedure is exactly the same, but the LHS of Eq. (4a) has the sign reversed. This procedure is similar to that used by Chang[3] or Salerno *et al.*[4] for a single drive term, or by Levring *et al.*[27] for asymmetric dc fields.

In Table I we also report some typical 2TOF cases: The map results are shown in Fig. 2, where they are compared with the analytical prediction. The agreement with the analytical prediction is satisfactory. Enhancement of the step sizes occurs only in the electric coupling case with $\sigma = 2$ at the fundamental frequency on the fundamental electric [FE; cf. Fig. 2(a)] step; this case corresponds to the small junction case of Monaco.[8]

The analogous situation on the fundamental magnetic (FM) step is totally different [cf. Fig. 2(b), crosses]; the amplitude gain is very small, the step becomes asymmetric, and becomes chaotic much earlier with respect to the single drive case [this is not shown in Fig. 2(b), but chaos is readily developed at the center of the steps]. We suggest that superharmonics of even order are not suitable for the biharmonic driving of a LJJ in the magnetic coupling case. On the other hand the behavior of a subharmonics step, i.e., $(1/2)M$ step [cf. Fig. 2(b), triangles], shows that, as expected (cf. previous section), this step is a 2TOF step also for $\eta_1 = 0$ with a very small amplitude. By pumping at a subharmonic of order 1/2, i.e., at the fundamental frequency, it can be strongly enhanced [cf. Fig. 2(b), stars].

In the general case of nTOF it is necessary to write n equations of n variables (θ, $T_1, T_2, ..., T_{n-1}$) and to find the zeros of this system. Though it is possible to find the nTOF solutions, here we do not follow this method but rather prefer to iterate the map. Ranges of the existence of typical steps with lowest order $n = 4$ are reported in Table I and shown in Fig. 3 (crosses denote the case of Ref. 23). From the figure it is clear that the steps, because of the biharmonic signal, lose in the range of PL symmetry and stability. Also in this case the biharmonic drive does not introduce a definitive enhancement.

Finally, we study numerically for the map the range of existence of other typical wave form signals. We consider triangular and square waves and two type of pulse trains: square and sawtooth (each with a pulse length which is 25% of the period). For all the signals the frequency was chosen to be the fundamental and the amplitudes of typical steps for sawtooth pulses are reported in Fig. 4. The ranges of PL steps are linear and identical both for square wave and triangular wave (electric or magnetic). For the pulse train the behavior is more complex: Positive pulses speed up the fluxon resulting in asymmetric steps that develop under the unperturbed curve, whereas negative pulses slow down the fluxon resulting in asymmetric steps above the unperturbed curve.

V. STABILITY ANALYSIS OF FIXED POINTS

Stability analysis for the 1TOF solutions with a single drive was carried out by Salerno *et al.*[4] for a biharmonic drive and with $\sigma = 1/2$, $\psi = \pi/4$ by Salerno.[12] Here we extend the analysis to the same system driven by a generic biharmonic (or wave form) drive. To determine the stability of the fixed points we follow the method

used in the standard stability analysis, i.e., to find the eigenvalues of the Jacobian evaluated in a fixed point and to impose the condition that the absolute values of the eigenvalues be less than 1. We find the following condition:

$$0 \leq \cos(\theta) + \sigma \frac{\eta_1}{\eta_0} \cos(\sigma\theta) \leq \frac{2(1+R)}{\omega\eta_0|F_u|}, \tag{12}$$

where R is the product of two eigenvalues for $\eta_0 = \eta_1 = 0$ and F_u is the derivative with respect to u of the first equation of the map [Eq. (4a)]. We note that there exists a negative slope part that is always unstable and a positive slope that becomes unstable above a certain value of the time derivative of the external signal. To visualize the modification of both the signal and its derivative we have plotted them in Fig. 5. For a given bias point, equivalent through Eq. (9) to a given amplitude of the signal, the corresponding stable points are those included in the region satisfying the inequality (12). For a given point of the step (i.e., a given bias value χ) there exist, depending on σ and η_1, several values of the phase that satisfy the condition (9). For some values of the phase the time derivatives of the two signals are added, and for some values they have opposite sign. In the latter case, for sufficiently high values of the subharmonic signal, a 2TOF state can be reduced to a 1TOF state. Generally speaking it is difficult to predict if the system will be stabilized or destabilized by the second term.

Since extremal points are always stable (the derivative of the signal vanishes), biharmonic signals having four extremal values instead of two will have four regions of stability instead of two (cf. Fig. 5). A *global* (see below) stabilization is realized if the images of the four stability regions on the θ axis, via the function $\eta(\theta)$, overlap.

Examples of stability regions in the parameter χ-η_1 plane for the typical cases of Table I are shown in Fig. 1 where we report also the results of numerical simulations with the map. The agreement is rather good, but there are several points (especially in the magnetic case) where the analysis predicts the existence and the stability of the fixed point, whereas the map exhibits annihilation of the fluxon (see Ref. 20 for a discussion of the meaning of fluxon annihilation in the map context), bifurcation, or chaos. We believe this is due to a shrinking of the 1TOF basin of attraction that coexists with a larger basin of attraction of the 2TOF or of the chaotic solutions. For instance, we have focused our attention on Fig. 1(c), for $\eta_1 = 0.05$ and $\chi \simeq 0.43$. Figure 6 shows the basins of attraction of the single TOF surrounded by the basin of attraction of the 2TOF. Indeed a very tiny basin of attraction of the 1TOF solution lies within the 2TOF basin but is so narrow (the width is less than 10^{-4}) that it cannot be shown on this scale. This phenomenon has not been observed for a single harmonic drive.

As we expected, the system is not always stabilized: In fact the second term can simply destroy the fluxon dynamics or, for certain values of the parameters, induce rather than suppress chaos. However, there are several examples of a *global* stabilization of the system [see Figs. 1(b) and 1(d)]; i.e., the chaotic regions on the step disappear. This occurs for values of η_1 that are about 20% or 30% of η_0: These are sufficiently large to stabilize the whole step, but yet not large enough to induce the breaking of the step in isolated stability regions surrounded by chaotic or annihilation regions. So, even though the added harmonic signal cannot give a great increase of

TABLE I. Step type and relative parameters for electric coupling (a) and for magnetic coupling (b); l' and k' are equal to the original l and k in the n-even magnetic case and are equal to $2l+1$ and $2k+1$ for the n-odd magnetic case. Step types are identified as E and M for the electric and magnetic cases, respectively [cf. Eqs. (7) and (8)]. A prefix indicates the order of subharmonic for the step with the simple harmonic signal ($\eta_1 = 0$); F indicates the step at the fundamental frequency.

(a)

E step	n	l	k	σ	ω
FE	1	1	2	2	V
$(1/2)E$	1	2	1	1/2	$2V$
FE	2	2	1	1/2	V
FE	2	2	4	2	V
FE	4	4	1	1/4	V

(b)

M step	n	l'	k'	σ	ω
FM	1	1	3	3	$V/2$
$(1/3)M$	1	3	1	1/3	$(3/2)V$
(1/3)M	1	3	5	5/3	$(3/2)V$
FM	2	1	2	2	$V/2$
$(1/2)M$	2	2	1	1/2	V
FM	4	2	1	1/2	$V/2$
$(1/3)M$	4	6	3	1/2	$(3/2)V$

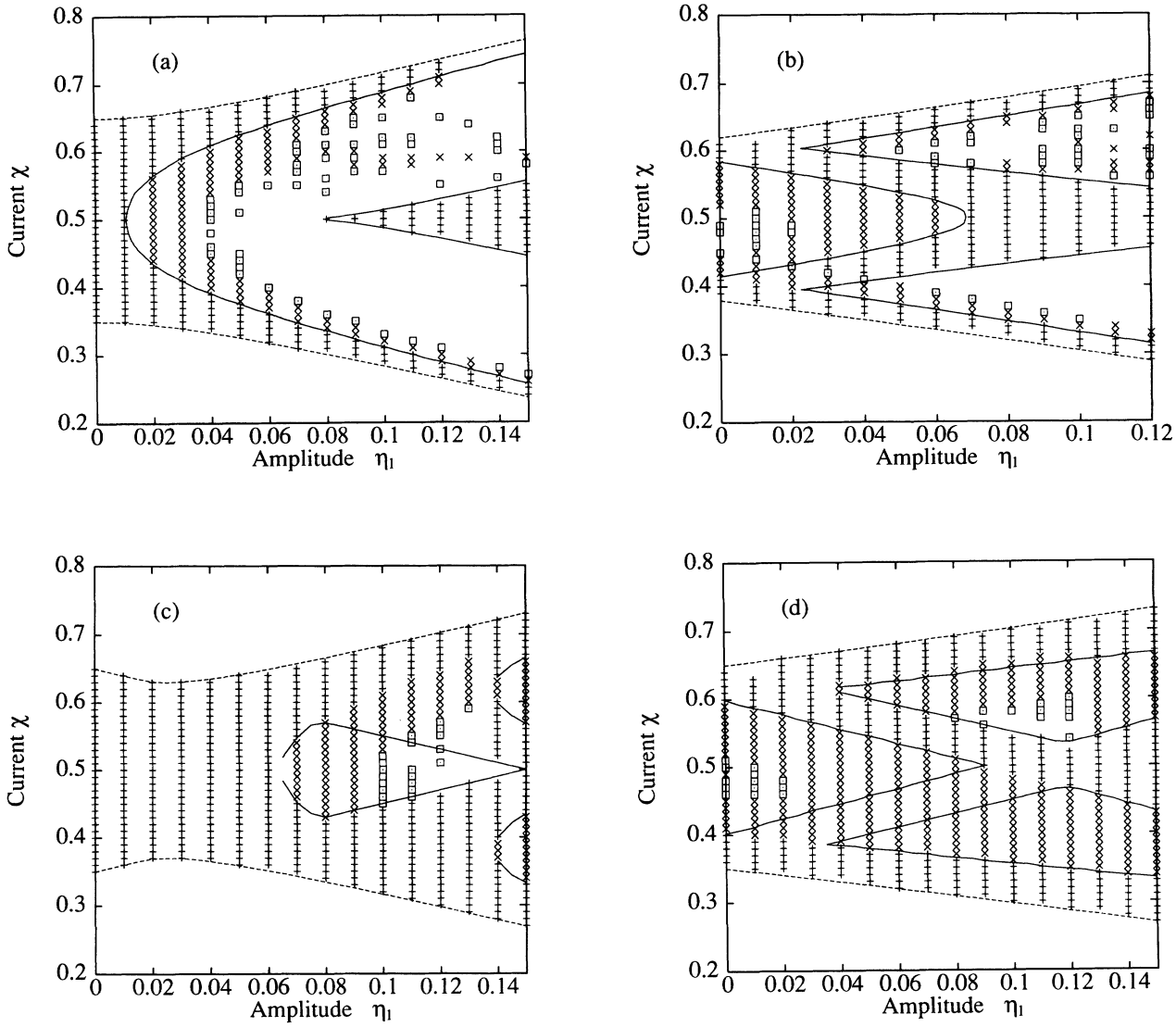

FIG. 1. Ranges of existence and stability of the nTOF solutions of the numerical solution as a function of the bias current and of the second harmonic amplitude for the following steps (reader can refer to Table I): (a) FE $\sigma = 2$, (b) $(1/2)E$ $\sigma = 1/2$, (c) FM $\sigma = 3$, (d) $(1/3)M$ $\sigma = 1/3$. In all the figures, + corresponds to the 1TOF solution, × corresponds to nTOF solutions, □ to chaotic solutions, and a blank to annihilation. Parameters of the junction are $L = 10$, $\alpha = 0.1$, $\beta = 0$. The dotted lines denote the range of existence of the step [Eq. (9)]. The solid lines denote the points where, according to the stability analysis [Eq. (12)], a bifurcation occurs.

locking range, a global stabilization effect will be produced.

A stability condition similar to (12) applies also for the stability of general wave forms by simply substituting the derivative of a biharmonic signal with the derivative of a generic wave form. To test this assumption we have investigated numerically triangular waves and sawtooth pulse trains. Results are perfectly consistent with the above assumption in the case of triangular waves; i.e., the transition between 1TOF and 2TOF solutions is independent of χ, as must also be for a triangular wave form. For a sawtooth pulse train the condition is substantially verified but some comments are needed: (i) From Fig. 4 we see a difference in amplitude between positive pulse and negative pulse; this is justified by the fact that the negative slope is always unstable as demonstrated above (a time-reversed sawtooth pulse having reversed slopes gives exactly the opposite result for positive and negative pulses); (ii) sawtooth pulse trains tend to develop chaos for large amplitudes in some regions of the step, whereas for triangular wave forms the bifurcation point, and so the chaos, is independent of χ according to the stability condition. We believe that this last point is related to the shape of the basins of attraction, in analogy with the case of two sinusoidal excitations (see Fig. 6).

Square waves, even more suitable in principle because

their derivative is always zero, do not show 1TOF solutions; many points on the square wave and square pulse train steps are affected by chaos or support solutions with a large number of TOF. A justification of this behavior can be traced to the following reason: For square wave forms an equation analogous to Eq. (9) cannot be written because the signal has only two values; therefore solutions with a small number of TOF cannot exist. In fact, in both square wave and square pulse trains, PL states are observed, but no 1TOF solutions seem to develop, though the steps for such small amplitudes remain vertical.

The same procedure could be applied to the second iterate of the map to stabilize the second bifurcation, i.e., to force the system from a period-4 solution to a period-2 solution, and so on, up to the critical point separating

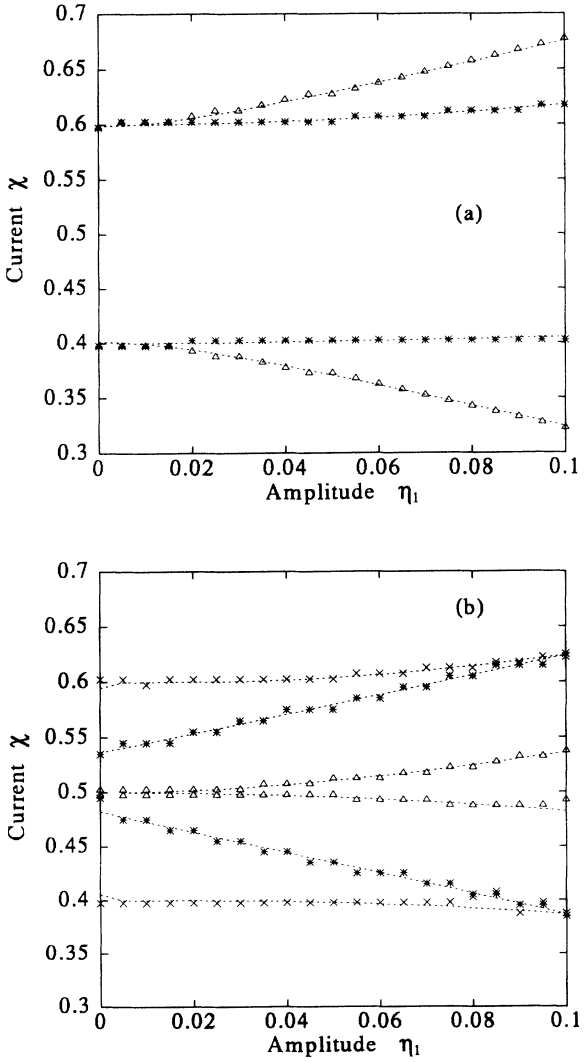

FIG. 2. Ranges of existence of the 2TOF solution: (a) electric, FE, $\sigma = 2$ ($\triangle$) and $\sigma = 1/2$ ($\star$); (b) magnetic, FM, $\sigma = 2$ ($\times$), and $(1/2)M$ both with single drive ($\triangle$) and biharmonic drive ($\star$). Readers can refer to Table I to identify other parameters of these steps. The dotted line refers to the range predicted by Eqs. (10) and (11). Parameters of the junction are $L = 10$, $\alpha = 0.1$, $\beta = 0$.

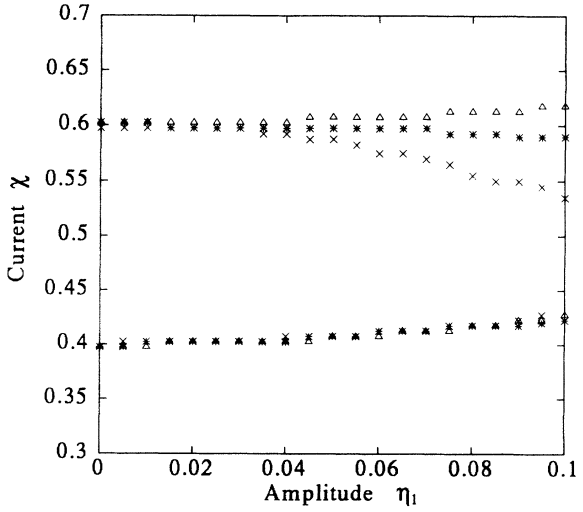

FIG. 3. Ranges of existence of the 4TOF solutions: FE, $\sigma = 1/4$ ($\star$); FM, $\sigma = 1/2$ ($\triangle$); $(1/3)M$, $\sigma = 1/2$ ($\times$). Reader can refer to Table I to identify other parameters of the steps. Parameters of the junction are $L = 10$, $\alpha = 0.1$, $\beta = 0$.

the cascade of bifurcations from chaos, where the chaos suppression occurs. The center of the step is again particularly illustrative of this mechanism. In this case, the required amplitude of the external drive being just zero, if one can choose a signal whose frequency allows the simple period 1 [1TOF solutions; see Eqs. (7) and (8)] and whose derivatives are subtracted, it is possible to obtain the full reverse Feigenbaum cascade, as observed in Ref. 23. Note that this phenomenon happens in all cases studied here [cf. Figs. 1(a), (b), (c), (d)] and the amplitude η_1 is not, in general, small with respect to η_0. Since an *exact* analysis of first bifurcation can be carried out

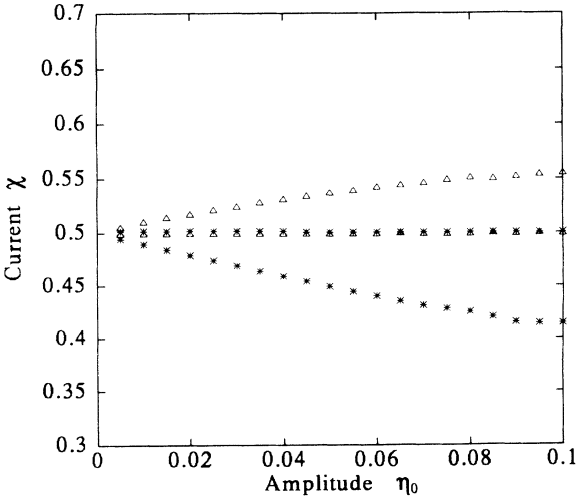

FIG. 4. Ranges for sawtooth pulse train ($\star$ indicates a positive amplitude; $\triangle$ indicates a negative amplitude). Parameters of the junction are $L = 10$, $\alpha = 0.1$, $\beta = 0$.

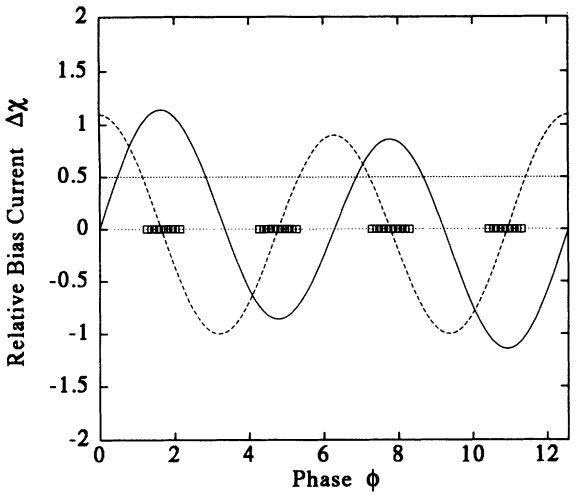

FIG. 5. Biharmonic signal (solid line) and its derivative (dotted line) for $\eta_1/\eta_0 = 0.2$. □ indicates the points where the derivative of the signal is below the threshold of Eq. (12) denoted by the solid horizontal line at $\Delta\chi = 0.5$. $\Delta\chi = \chi - \chi_0$, where χ_0 is the bias current at the center of the step.

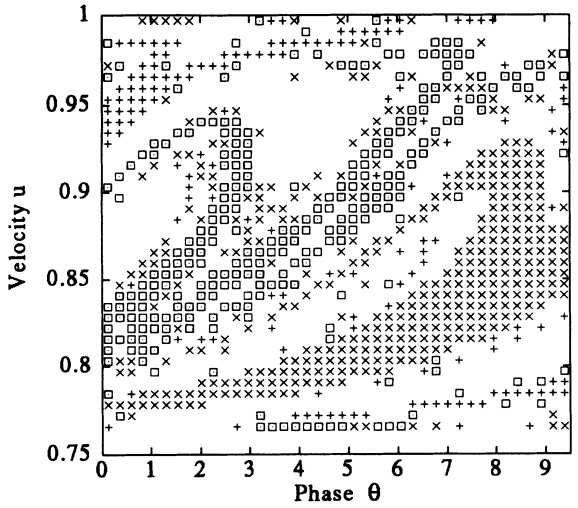

FIG. 6. Basins of attraction of the solution for $\chi = 0.43$, $\eta_0 = 0.15$, $\eta_1 = 0.05$, $L = 10$, $\alpha = 0.1$, $\beta = 0$. + corresponds to the 1TOF solution, × corresponds to 2TOF solutions, □ to multiple TOF and chaotic solutions. A blank refers to annihilation. Fixed point with the tiny 1TOF attraction basis is within the large 2TOF basin.

in particular for the center of the step, one can predict if chaos suppression at the center of the step is achieved for large or small values of η_1/η_0.

VI. CONCLUSION

The case of two sinusoidal excitations in a LJJ is an important example of a system driven by two periodic signals because it allows an analytical treatment of at least the first bifurcation. We note that most of the considerations done for such a case are of general relevance. In particular, the prescriptions for the frequencies are valid also in the case of a short junction, and can be applied in principle to any nonlinear oscillator (a Van der Pol oscillator, for example).

For this system we have found that the use of a second harmonic might improve the stability and enhance the amplitude of the phase locked states if (i) the frequency of the second harmonic is appropriate; (ii) the sum of the derivatives of the two signals is less than the derivative of the single harmonic signal for a given bias point. In contrast with the spirit of the OGY method (stabilization of unstable orbits) we have shown that the use of a second periodic signal drastically changes the structure and the number of the fixed points. Moreover, they induce a drastic change in the form of the basin of attraction even for very small values of the amplitude of the second harmonic. The method will be successful only if an appropriate choice of both the external frequency and amplitude is made. The stability results can be applied to systems described by any parametric two-dimensional map which describe systems that show phase-locked states, but for continuous systems (such as the small Josephson junctions or the Van der Pol oscillator), even if a Poincaré map can be imagined, the use of the prescriptions is more complicated: In this case the oscillating term acts continuously on the system and conditions as those stated in Eq. (9) and Eq. (12) are not easily translated for such systems. We nevertheless believe that the basic mechanism (two signals that sum to the same effective amplitude but with a different stability region) is obviously the same, as is intuitively clear from Ref. 24. The conditions here derived may serve as a starting point, and it has to be demonstrated to what extent they can be applied to continuous systems. Surprisingly, the full PDE system, in principle more complicated, is for its peculiar form well described by this approach.[23]

ACKNOWLEDGMENTS

We wish to acknowledge R.D. Parmentier for a critical reading of the manuscript. We had many helpful discussions and suggestions with M. Salerno and R. Monaco, to whom goes our gratitude. Financial support from MURST (Italy), from the Progetto Finalizzato "Tecnologie Superconduttive e Criogeniche" del CNR (Italy), and from the EU Esprit Project (Contract No. 7100) is gratefully acknowledged.

[1] G. Costabile *et al.*, Jpn. J. Appl. Phys. **26**, 1639 (1987); G. Costabile, R. Monaco, and S. Pagano, J. Appl. Phys. **63**, 5406 (1988).

[2] R.D. Parmentier, in *The New Superconducting Electronic*, edited by H. Weinstock and R.W. Ralsten (Kluwer, Dordrecht, 1993), p. 221.

[3] J.J. Chang, Phys. Rev. B **34**, 6137 (1986).

[4] M. Salerno, M.R. Samuelsen, G. Filatrella, S. Pagano, and

R.D. Parmentier, Phys. Rev. B **41**, 6641 (1990).
[5] A. Barone and G. Paternó, *Physics and Applications of Josephson Effect* (Wiley, New York, 1982).
[6] G. Costabile, R. Monaco, S. Pagano, and G. Rotoli, Phys. Rev. B **42**, 2651 (1990).
[7] G. Filatrella, G. Rotoli, N. Grøenbech-Jensen, R.D. Parmentier, and N.F. Pedersen, J. Appl. Phys. **72**, 3179 (1992).
[8] R. Monaco, J. Appl. Phys. **68**, 679 (1990).
[9] K. Wiesenfeld and P. Bryant, Phys. Rev. A **33**, 2545 (1986).
[10] B. Svensmark and M.R. Samuelsen, Phys. Rev. B **41**, 4181 (1990).
[11] Y. Braiman and I. Goldhirsch, Phys. Rev. Lett. **66**, 2545 (1991).
[12] M. Salerno, Phys. Rev. B **44**, 2720 (1991).
[13] R.L. Kautz, in *Structure, Coherence and Chaos in Dynamical Systems,* edited by Peter L. Christiansen and R.D. Parmentier (Manchester University Press, Manchester, 1989); R.L. Kautz and R. Monaco, J. Appl. Phys. **57**, 875 (1985).
[14] A.R. Bishop, D.W. McLaughlin, M.G. Forest, and E.A. Overman II, Phys. Lett. A **127**, 335 (1988); A.R. Bishop, M.G. Forest, D.W. McLaughlin, and E.A. Overman II, Physica D **23**, 293 (1986).
[15] L.E. Guerrero and M. Octavio, Phys. Rev. A **37**, 3641 (1988); **40**, 3371 (1989).
[16] M. Cirillo, A.R. Bishop, N. Grøenbech-Jensen, and P.S. Lomdahl, Phys. Rev. E **49**, 3606 (1994).
[17] F.K. Abdullaev and N.A. Khikmatov, Sov. Phys. Tech. Phys. **30**, 561 (1985).
[18] W.J. Yeh, O.G. Symko, and D.J. Zheng, Phys. Rev. B **42**, 4080 (1990).
[19] G. Rotoli and G. Filatrella, Phys. Lett. A **156**, 211 (1991).
[20] G. Filatrella and G. Rotoli, J. Phys. A **26** 4937 (1993); G. Rotoli and G. Filatrella, in *Proceedings of VII Interdisciplinar Workshop "Nonlinear Coherent Effects in Physics and Biology,"* edited by M. Peyrard and M. Remoissenet (Springer-Verlag, Berlin, 1991), p. 284.
[21] E. Ott, C. Grebogi, and J.A. Yorke, Phys. Rev. Lett. **64**, 1196 (1990).
[22] S. Rajasekar and M. Lakshmann, Physica D **67**, 282 (1993).
[23] G. Filatrella, G. Rotoli, and M. Salerno, Phys. Lett. A **178**, 81 (1993).
[24] G. Cicogna and L. Fronzoni, Phys. Rev. E **47**, 4585 (1993).
[25] D.W. McLaughlin and A.C. Scott, Phys. Rev. A **18**, 1652 (1978).
[26] G. Filatrella, G. Rotoli, and R.D. Parmentier, Phys. Lett. A **148**, 122 (1990).
[27] O.A. Levring, N.F. Pedersen, and M.R. Samuelsen, J. Appl. Phys. **54**, 987 (1983).